similar results for line shape and power absorbed. We also have found that when the rf frequency is swept by keeping H_0 fixed, the shift of the peak position for thicker samples is to lower frequencies, for both calculations. This is contrary to the graphs given in Ref. 2.

In conclusion, CESR in superconductors is at least theoretically possible and would be experimentally easier the higher the critical field since the power absorbed $P_M \propto H_0^2$ and also since the signal-to-background ratio $H_s/H_b \propto H_0$.

ACKNOWLEDGMENTS

We are grateful to M. P. Garfunkel, F. M. Lurie, and A. Yelon for useful discussions.

*Research supported in part by a grant from the National Science Foundation.

[1]S. Schultz, G. Dunifer, and C. Latham, Phys. Letters 23, 192 (1966).
[2]J. I. Kaplan, Phys. Letters 19, 266 (1965).
[3]F. J. Dyson, Phys. Rev. 98, 349 (1955).
[4]M. Lampe and P. M. Platzman, Phys. Rev. 150, 340 (1966).
[5]W. M. Walsh, Jr., L. W. Rupp, Jr., and P. H. Schmidt, Phys. Rev. 142, 414 (1966).
[6]J. Bardeen, L. N. Cooper, and J. R. Schrieffer, Phys. Rev. 108, 1175 (1957).
[7]N. N. Bogoliubov, Nuovo Cimento 7, 794 (1958).
[8]J. Millstein and M. Tinkham, Phys. Rev. 158, 325 (1967).

PHYSICAL REVIEW B VOLUME 2, NUMBER 7 1 OCTOBER 1970

Breakdown of the Mean Field Theory in the Superconducting Transition Region

J. P. Hurault* and K. Maki†

Laboratoire de Physique des Solides‡ Faculté des Sciences 91-Orsay, France

(Received 26 January 1970)

We consider a dirty superconducting material above its transition temperature. Using a perturbation expansion, we study the effect of the fluctuations of the order parameter on the electron Green's function G as well as on the fluctuation Green's function $\mathfrak{D}$. Our main results are : (a) G and $\mathfrak{D}$ can be determined separately. (b) The behavior of $\mathfrak{D}$ can be analyzed using the Ginzburg-Landau functional where the only nonlinear term present is the lowest-order one. (c) As a result of this analysis, the corrections to the mean field theory are generally small as far as $\mathfrak{D}$ is concerned. They become important only at the onset of the critical region, where our perturbation approach breaks down. We derive a criterion for the onset of this critical region and compare our estimate to previous ones. (d) On the other hand, G is well described by taking only the lowest-order correction to the electron self-energy due to the fluctuations, even inside the critical region. (e) We propose a scheme for the analysis of the critical region. (f) We establish in this way the complete equivalence between the critical behavior of the interacting Bose system and that of a superconductor.

I. INTRODUCTION

The fluctuations of the order parameter in "dirty" one- or two-dimensional superconductors (thin films or whiskers) have been studied extensively both theoretically and experimentally.[1–15] Many experiments on the electrical conductivity[2,3] seem to be successfully accounted for in terms of the Aslamazov-Larkin theory,[9] which is a mean field approach, although there exists still a question about the completeness of that derivation.[11,13]

On the other hand, there has been a number of suggestions[16–23] that the mean field theory will be no longer valid in the immediate vicinity of the transition temperature, where the fluctuation spectrum of the order parameter may be modified drastically.

In the present work, we use a perturbation expansion technique to study systematically the effect of the fluctuations of the order parameter on the electron Green's function G as well as on the fluctuation Green's function $\mathfrak{D}$. As a preparation of a more complete analysis, we start with a study of the first-order correction to G (Sec. II) and to $\mathfrak{D}$ (Sec. III). We find that the effect of the first-order correction is much more important on $\mathfrak{D}$ than on G. A detailed analysis of the higher-order corrections are carried out in Sec. IV, which results in the following conclusions.

(a) G and $\mathfrak{D}$ can be determined separately.

(b) The behavior of $\mathfrak{D}$ can be analyzed using the Ginzburg-Landau functional where the only nonlinear term present is the lowest-order one.

(c) As far as G is concerned, the self-energy Σ due to the fluctuations of the order parameter is yielded by the following expansion:

$$\Sigma = \sum_{n=1}^{\infty} c_n x_i^n , \tag{1.1}$$

where $x = x_i$ ($i = 3, 2, 1$) depends on the dimensionality of the sample. Thus, in the three-dimensional case

$$x_3 = 1/l\xi p_0^2 . \tag{1.2}$$

In the two-dimensional case (a film of thickness d)

$$x_2 = (1/p_0^2 ld)\ln(1/\eta) . \tag{1.3}$$

In the one-dimensional case (a whisker of cross section d^2)

$$x_1 = (\xi/p_0^2 ld^2)\eta^{-1/2} . \tag{1.4}$$

In the above relations, the c_n are coefficients of order $1/\tau$,[24] τ being the mean collision time; l is the mean free path, p_0 is the Fermi wave vector, ξ is the coherence length of a dirty superconductor [i.e., $\xi = (\xi_0 l)^{1/2}$], and η is given by

$$\eta = \ln(T/T_c) \sim (T - T_c)/T_c , \tag{1.5}$$

since we are close to T_c.

The above relations have been obtained using for $\mathfrak{D}$ the expression $\mathfrak{D}_0$ obtained by the mean field approximation

$$\mathfrak{D}_0(\omega_\nu, q) = [1/N(0)][(\pi/8T)|\omega_\nu| + \eta + \lambda q^2]^{-1} . \tag{1.6}$$

In (1.6), $N(0) = mp_0/2\pi^2$ is the density of states at the Fermi level

$$\lambda = (\pi/8T)D, \quad D = lp_0/3m$$

being the diffusion constant of our dirty material.

(d) As far as $\mathfrak{D}$ is concerned, the self-energy corrections to the fluctuation propagator, $\delta\eta$, are also yielded by a power expansion such as

$$\delta\eta/\eta = \sum_n b_n y_i^n , \tag{1.7}$$

where the b_n are coefficients of the order of one. Depending on the dimensionality, we have

$$y_3 = (1/p_0^2 l\xi)\eta^{-1/2} , \tag{1.8}$$

$$y_2 = (1/p_0^2 ld)\eta^{-1} , \tag{1.9}$$

$$y_1 = (\xi/ld^2 p_0^2)\eta^{-3/2} . \tag{1.10}$$

(e) From the consideration of points (c) and (d), it is clear that, in the analysis of the critical behavior of the system, we can neglect the modifications of the electronic Green's function due to the fluctuations. It is sufficient to concentrate on the modifications of the fluctuation Green's function using the Ginzburg-Landau functional. The modifications of G are in terms appropriately described if one retains only the first-order corrections due to the fluctuations, provided that the proper $\mathfrak{D}$ is inserted in the calculation.

Consequently, we establish that the critical behavior in a superconductor is equivalent to that in the interacting Bose system as far as the thermodynamical (or equilibrium) properties are concerned. On the other hand, let us point out that this equivalence does not necessarily hold for dynamic transport properties such as the conductivity mentioned above.

(f) We define the onset of the critical region (i.e., the breakdown of the mean field theory) by the condition $y \simeq 1$. Depending on the dimension, this criterion can also be written $\eta = \eta_{c_i}$. Thus

$$\eta_{c3} = 1/(p_0 l)^3 \xi_0 p_0 , \tag{1.11}$$

$$\eta_{c2} = 1/p_0^2 ld , \tag{1.12}$$

$$\eta_{c1} = [\xi_0/(p_0 d)^4 l]^{1/3} ,$$

Our criteria agree with estimates made in Refs. 16 and 20–22 but disagree with estimates resulting from Refs. 17 and 18. In the two-dimensional case, the condition (1.12) gives a good account for the deviation of the electrical conductivity from the $T_c/(T-T_c)$ law in the immediate vicinity of T_c as observed by Glover.[2] On the other hand, the present result cannot explain the thickness dependence of the shift in T_c observed in the same experiments.[25] Indeed, the estimate from the fluctuation effect gives a shift by a factor of 10 smaller than that observed. This implies the existence of another cause, such as a proximity effect as pointed out in Ref. 26.

Finally, as a byproduct, we derive the expression of the tunneling density of states where an additional structure due to the fluctuations is present. This expression agrees with a result obtained by Abrahams, Redi, and Woo,[15] and also accounts for the experiments carried out by Cohen, Abeles, and Fuselier.[5]

II. CORRECTIONS TO ELECTRON GREEN'S FUNCTION G

In the absence of any impurity, we start with the following Hamiltonian:

$$\mathcal{H} = \sum_{p\sigma} \xi_p a_{p\sigma}^\dagger a_{p\sigma} + \sum_{p,q} (\psi_q^\dagger a_{p+q,\uparrow} a_{-p,\downarrow} + \psi_q a_{p+q,\uparrow}^\dagger a_{-p,\downarrow}^\dagger) , \tag{2.1}$$

where $a_{p\sigma}^\dagger$ and $a_{p\sigma}$ are the electron creation and annihilation operators, respectively, $\xi_p = p^2/2m - \mu$ is the energy of the electron measured from the Fermi level. $\psi_q^\dagger$ is such that

$$\psi_q^\dagger = |g| \sum_p a_{p+q,\uparrow}^\dagger a_{-p,\downarrow}^\dagger , \tag{2.2}$$

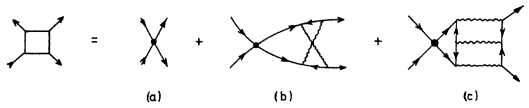

FIG. 1. Diagrammatic representation of the vertex corrections. The diagram (a) is the zeroth-order vertex.

$|g|$ being the BCS interaction.

The correlation function of the order parameter (i.e., the Green's function for $\psi_q^\dagger$) is determined by

$$\langle T[\psi_q^\dagger(t)\psi_q(0)]\rangle_{\omega_\nu} = \frac{|g|^2\Pi(q,\omega_\nu)}{1-|g|\Pi(q,\omega_\nu)}\,, \tag{2.3}$$

where

$$\Pi(q,\omega_\nu) = T\sum_n \int \frac{d^3p}{(2\pi)^3}\,\square(\vec{p}+\vec{q},\omega_n+\omega_\nu;-\vec{p},-\omega_n) \times G(\omega_n+\omega_\nu,\vec{p}+\vec{q})\,G(-\omega_n,-\vec{p})\,. \tag{2.4}$$

Here $G(\omega_n,\vec{p})$ is the renormalized Green's function of the electron and $\square$ is the irreducible vertex. $\square$ is given by a diagrammatic expansion (see Fig. 1), for example. In Fig. 1, the wavy lines correspond to the fluctuation Green's function $\mathfrak{D}$ while the straight lines correspond to G. In first approximation, $\square$ is given by Fig. 1(a).

On the other hand, the electron Green's function is given by the following expression:

$$G(\vec{p},\omega_n)^{-1} = G_0(\vec{p},\omega_n)^{-1} - \Sigma(\vec{p},\omega_n)\,. \tag{2.5}$$

In (2.5), G_0 is the electron Green's function in the absence of fluctuations.

Now, we limit our considerations to "dirty" superconductors, where the electron mean free path is much shorter than the coherence length. The relevant average on the randomized scattering centers can be achieved according to the standard technique.[27] Thus, in standard notations

$$G_0(\vec{p},\omega_n) = (i\tilde{\omega}_n - \xi)^{-1}$$

with

$$\tilde{\omega}_n = \omega_n(1+1/2\tau|\omega_n|)\,. \tag{2.6}$$

The self-energy $\Sigma(\vec{p},\omega_n)$ is given by the diagrammatic expansion shown in Fig. 2. In Fig. 2, the dotted line corresponds to the scattering of the electrons on the impurities.

Now, we want to evaluate the lowest-order terms in $\Sigma(\vec{p},\omega_n)$. This is obtained by the summation of Figs. 2(a) and 2(b). If Σ_a denotes the contribution of Fig. 2(a) to $\Sigma(\vec{p},\omega_n)$, then Σ_a is given by

$$\Sigma_a(\vec{p},\omega_n) = T\sum_\nu\sum_q[\Lambda(\omega_n,\omega_{n+\nu},\vec{q})]^2 \times \mathfrak{D}(-\vec{q},\omega_\nu)G_0[\vec{p}+\vec{q},-(\omega_{n+\nu})]\,, \tag{2.7}$$

where

$$\Lambda(\omega_n,\omega_{n+\nu};\vec{q}) = \frac{|2\omega_n+\omega_\nu|+\tau^{-1}}{|2\omega_n+\omega_\nu|+Dq^2} \quad \text{for } \omega_n\cdot\omega_{n+\nu}>0$$
$$= 1 \quad \text{for } \omega_n\cdot\omega_{n+\nu}<0\,, \tag{2.8}$$

$$\mathfrak{D}(\vec{q},\omega_\nu) = \frac{1}{N(0)}\,\frac{1}{\eta+\lambda q^2+\pi|\omega_\nu|/8T_c}\,. \tag{2.9}$$

We recall also that $\omega_n = (2n+1)\pi T$ and that $\omega_\nu = 2\nu\pi T$. In a dirty material ($2\pi T_c\tau \ll 1$), Eq. (2.7) can be reasonably approximated by

$$\Sigma_a(\vec{p},\omega_n) \simeq G_0(\vec{p},-\omega_n)F(|\omega_n|)\,. \tag{2.10}$$

This separation is possible, since the momentum involved in the fluctuation propagator (which is of the order of the inverse of the temperature-dependent coherence length) is much smaller than the momentum characteristic of the conduction electrons p_0 (see also Ref. 15).

After the summation over ν, $F(|\omega_n|)$ is yielded in terms of digamma functions. In view of the summation over q, it is sufficient to replace $\psi(z)$ by its expression for small arguments, i.e., $-1/z$. Finally, keeping the most important terms, we can write (see the Appendix)

$$F(|\omega_n|) \simeq (2\tilde{\omega}_n)^2\frac{8T^2}{\pi N(0)}\sum_{\vec{q}}\left[\frac{1}{(|2\omega_n|-\epsilon)^2}\left(\frac{1}{\epsilon+Dq^2}-\frac{2}{(\epsilon+|2\omega_n|+2Dq^2}\right)-\frac{2}{(|2\omega_n|-\epsilon)}\,\frac{1}{(\epsilon+|2\omega_n|+2Dq^2)^2}\right]. \tag{2.11}$$

The summation over $\vec{q}$ results in

$$F(|\omega_n|) \simeq \tilde{\omega}_n^2\,A_i(|\omega_n|)\,, \tag{2.12}$$

depending on the dimension. Thus

$$A_3(|\omega_n|) = \left(\frac{2T}{\pi}\right)^2\frac{1}{N(0)D\xi(T)}\,\frac{2}{(2|\omega_n|-\epsilon)^2} \times\left(\frac{\frac{3}{2}+|\omega_n|/\epsilon}{(2+4|\omega_n|/\epsilon)^{1/2}}-1\right), \tag{2.13}$$

$$A_2(|\omega_n|) = \left(\frac{2T}{\pi}\right)^2\frac{1}{N(0)Dd}\,\frac{2}{(|2\omega_n|-\epsilon)^2} \times\left[\ln\left(\frac{|\omega_n|}{\epsilon}+\frac{1}{2}\right)-\frac{|2\omega_n|-\epsilon}{|2\omega_n|+\epsilon}\right], \tag{2.14}$$

$$A_1(|\omega_n|) = \left(\frac{2T}{\pi}\right)^2\frac{\pi\xi(T)}{N(0)Dd^2}\,\frac{4}{(|2\omega_n|-\epsilon)^2} \times\left(1-\frac{3|\omega_n|+\frac{1}{2}\epsilon}{|2\omega_n|+\epsilon}\,\frac{1}{(2+4|\omega_n|/\epsilon)^{1/2}}\right). \tag{2.15}$$

In (2.13)–(2.15), $\xi(T)$, the temperature coherence length, is such that

$$\xi(T)=(D/\epsilon)^{1/2} \quad \text{with } \epsilon=(8T/\pi)\eta \ . \tag{2.16}$$

Now, the consideration of Fig. 2(b) yields for Σ_b

$$\Sigma_b = n\int \frac{d^3p'}{(2\pi)^3}\frac{|u(\theta')|^2}{(i\tilde{\omega}_n-\xi_{p'})^2}\frac{F(\omega_n)}{i\tilde{\omega}_n+\xi_{p'}}$$
$$\simeq (i/4\tau)\,\mathrm{sign}(\omega_n)A(|\omega_n|) \ . \tag{2.17}$$

Hence $\Sigma=\Sigma_a+\Sigma_b$ is such that

$$\Sigma \simeq \left(\frac{\tilde{\omega}_n^2}{i\tilde{\omega}_n+\xi}+\frac{i\,\mathrm{sign}\omega_n}{4\tau}\right)A(|\omega_n|)$$
$$\simeq \frac{i\tilde{\omega}_n-\xi}{i\tilde{\omega}_n+\xi}\left[-\tfrac{1}{2}i\tilde{\omega}_n A(|\omega_n|)\right] . \tag{2.18}$$

In (2.17), n is the number of impurities per unit volume and u is the impurity potential. Finally, within the present approximation, the renormalized Green's function is given by

$$G(\vec{p},\omega_n)=\left\{i\tilde{\omega}_n-\xi-\frac{i\tilde{\omega}_n-\xi}{i\tilde{\omega}_n+\xi}\left[-\tfrac{1}{2}i\tilde{\omega}_n A(|\omega_n|)\right]\right\}^{-1}$$
$$=\frac{i\tilde{\omega}_n+\xi}{(i\tilde{\omega}_n-\xi)\{i\tilde{\omega}_n[1+\frac{1}{2}A(|\omega_n|)]+\xi\}} \ . \tag{2.19}$$

The above expressions for $A(|\omega_n|)$ result in an anomalous behavior of the tunneling density of states, as observed experimentally by Cohen, Abeles, and Fuselier.[5] From (2.13)–(2.15), we can deduce the value of this anomalous component. Thus, if $\nu(\omega)=[N(\omega)-N_N(\omega)]/N_N(0)$, $N(\omega)$ being the total density of states and N_N the density of states when the fluctuations are not taken into account,

$$\nu_3(\omega)=\left(\frac{2T}{\pi}\right)^2\frac{2}{N(0)D\xi(T)}$$
$$\times\mathrm{Re}\left[-\frac{1}{(2i\omega+\epsilon)^2}\left(\frac{\frac{3}{2}-i\omega/\epsilon}{(2-4i\omega/\epsilon)^{1/2}}-1\right)\right] , \tag{2.20}$$

$$\nu_2(\omega)=\left(\frac{2T}{\pi}\right)^2\frac{2}{N(0)Dd}\,\mathrm{Re}\frac{1}{(2i\omega+\epsilon)^2}$$
$$\times\left\{\left[\ln\left(\frac{-i\omega}{\epsilon}+\frac{1}{2}\right)-\frac{2i\omega+\epsilon}{2i\omega-\epsilon}\right]\right\} . \tag{2.21}$$

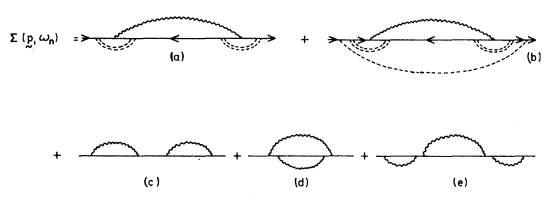

FIG. 2. Diagrammatic representation of the electronic self-energy.

A similar result has been obtained by Abrahams, Redi, and Woo.[15] Although these authors neglected the contribution of Fig. 2(b) in the calculation of the self-energy Σ, they found the same density of states, since in the local quantity associated with the single-particle Green's function like the density of states, Σ_b does not contribute because Σ_b can be viewed as the density vertex correction with a large momentum transfer. On the other hand, in the consideration of the self-energy correction to D (which is discussed in Sec. III) we cannot neglect Fig. 2(b).

In the consideration of the thermodynamical properties where $|\omega_n|$ is always much larger than ϵ, we can further approximate $A(|\omega_n|)$ by

$$A_3(|\omega_n|)\simeq\left(\frac{T}{\pi}\right)^2\frac{1}{N(0)D\xi(T)}\frac{1}{|\omega_n|^2}\left(\frac{|\omega_n|}{\epsilon}\right)^{1/2} , \tag{2.22}$$

$$A_2(|\omega_n|)\simeq\left(\frac{T}{\pi}\right)^2\frac{1}{N(0)Dd}\frac{2}{|\omega_n|^2}\left[\ln\left(\frac{|\omega_n|}{\epsilon}\right)-1\right] , \tag{2.23}$$

$$A_1(|\omega_n|)\simeq\left(\frac{2T}{\pi}\right)^2\frac{\pi\xi(T)}{N(0)Dd^2}\frac{1}{|\omega_n|^2} \ , \tag{2.24}$$

and, apart from numerical factors, the A_i can be identified to the x_i defined in (1.2)–(1.4).

We note also that the above results [i.e., Eqs. (2.22)–(2.24)] are more simply obtained by neglecting completely the summation over frequencies in the calculation of $\Sigma(\omega_n)$ and retaining only the fluctuation with $\omega_\nu=0$, associated with $\mathfrak{D}(0,\vec{q})$. In other words, in the analysis of the thermodynamical properties (or equilibrium properties), it is sufficient to consider the effect of the fluctuations of the order parameter with $\omega_\nu=0$ only.

We shall conclude this section with a discussion of the higher-order corrections to the electron Green's function, as are represented, for example, by Figs. 2(c)–2(e). Since the momenta involved in the propagator of the fluctuation are of the order of $\xi^{-1}(T)=(\lambda/\eta)^{1/2}$, while the momenta in the electron Green's function are of the order of p_0, we can always perform the integrals over the momenta in the fluctuation propagator separately. It is then easy to notice that the higher-order terms give rise to corrections in higher order in x_i, where the quantity x_i is defined in (1.2)–(1.4).

However, we will see in the next sections that the effect of the higher-order terms is extremely small, in the case of G, compared to those in the correction of $\mathfrak{D}$.

III. FIRST-ORDER CORRECTIONS TO $\mathfrak{D}$

To zeroth order, i.e., when the self-energy and vertex corrections are neglected, the quantity $\Pi(q,\omega_\nu)$ is yielded by the diagram (α) of Fig. 3,

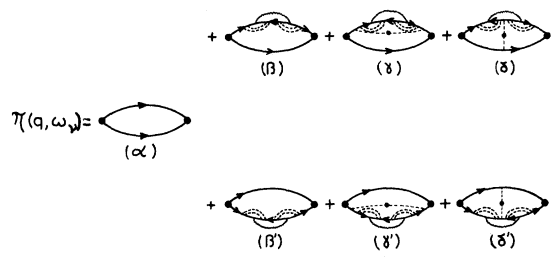

FIG. 3. Diagrammatic representation for the quantity $\Pi(q, \omega_\nu)$ entering the calculation of the fluctuation Green's function. The diagram (α) is associated to the mean field theory expansion for Π and the diagrams β, γ, δ, β', γ', δ' are associated to the first-order corrections.

which results, from (2.3) and (2.4), in the expression (1.6) for $\mathfrak{D}$. This is the expression adopted, for example, by Caroli and Maki.[28]

Now, we go one step further and sum all the first-order corrections for $\Pi(q, \omega_\nu)$. In such a case, Π is yielded by the sum of diagrams represented in Fig. 3.

Each diagram can be easily evaluated using the same technique as previously. Summing all of them, we have (see the Appendix)

$$\Pi(q, \omega_\nu) \simeq 2\pi T N(0) \times \sum_{n \geq 0}^{\omega_D/2\pi T} \left(\frac{1}{\omega_n + \frac{1}{2}\omega_\nu + \frac{1}{2} Dq^2} [1 + A(|\omega_n|)] \right) . \tag{3.1}$$

From (3.1), (2.3), and (2.4), we can deduce $\mathfrak{D}(q, \omega_\nu)$. Assuming

$$\mathfrak{D}(q, \omega_\nu) = \frac{1}{N(0)} \frac{1}{\tilde{\eta} + \tilde{\lambda} q^2 + \pi |\omega_\nu| / 8T} , \tag{3.2}$$

we obtain the following relations:

$$\tilde{\eta} = \eta + 2\pi T \sum_{n>0}^{\infty} \frac{1}{|\omega_n|} A(|\omega_n|) , \tag{3.3}$$

$$\tilde{\lambda} = \lambda \left(1 - 8T^2 \sum_{n \geq 0}^{\infty} \frac{1}{|\omega_n|^2} A(|\omega_n|) \right) . \tag{3.4}$$

We did not consider here the dynamical corrections to $\mathfrak{D}$ (i.e., the modification of the coefficient of $|\omega_\nu|$ in $\mathfrak{D}$) for two reasons: First, because the lowest-order term considered here [i.e., $\Pi(\vec{q}, \omega_\nu)$ given in (3.1)] is practically independent of ω_ν so that $\Pi(\vec{q}, \omega_\nu) \simeq \Pi(\vec{q}, 0)$, the second, because we are only interested in the following in the equilibrium properties of the system. In this situation we can assume in practice $|\omega_\nu| \gg \epsilon_0$ for $\nu \neq 0$ to a good approximation. Then the most important correction appears only in $\mathfrak{D}(\vec{q}, 0)$ while the corrections to $\mathfrak{D}(\vec{q}, \omega_\nu)$ (for $\nu \neq 0$) are always negligible. On the other hand, it will be worthwhile to point out that in the discussion of the dynamical properties, we cannot neglect the dynamical corrections mentioned above. Furthermore, the problem may be much more complicated due to the appearance of the new singularity associated with the vertex renormalization of the scalar potential term as has first pointed out by Gor'Kov and Eliashberg.[29] We point out also that the correction to $\tilde{\lambda}$ given in (3.4) is practically negligible. In fact a more important correction to $\tilde{\lambda}$ comes from the next-order correction in the fluctuation (see Sec. IV).

In fact, the correction term can also be expressed in powers of the y_i already defined in Sec. I. This behavior differs completely from what Kadanoff and Laramore had predicted from a phenomenological analysis.[23]

Using (2.22)–(2.24), we can write three different expressions for $\tilde{\eta}$, depending on the dimension of the system,

$$\tilde{\eta}_3 = \eta \left(1 + \frac{\zeta(\frac{5}{2})}{\pi^4} (\sqrt{2} - \tfrac{1}{4}) \frac{\sqrt{(2\pi)}}{N(0) D \xi(0)} \frac{1}{\eta} \right) , \tag{3.5}$$

$$\tilde{\eta}_2 = \eta \left(1 + \frac{7\zeta(3)}{2\pi^4} \frac{1}{N(0) Dd} \frac{\ln(\eta^{-1})}{\eta} \right) , \tag{3.6}$$

$$\tilde{\eta}_1 = \eta \left(1 + \frac{7\zeta(3)}{\pi^3} \frac{\xi(0)}{N(0) D d^2} \frac{1}{\eta^{3/2}} \right) . \tag{3.7}$$

In (3.5) and (3.7), $\xi(0) = (\pi D / 8T)^{1/2}$.

The graphical representation of $\tilde{\eta}_1$, $\tilde{\eta}_2$, $\tilde{\eta}_3$ as a function of η can be qualitatively seen in Fig. 4. If, in the three-dimensional case, the first-order corrections we have considered result in a finite shift in η, those corrections become divergent in

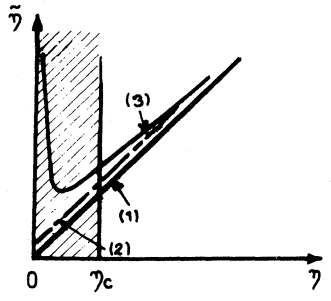

FIG. 4. Schematic representation of the renormalized η, $\tilde{\eta}$, as a function of η. The renormalization effects are due to the first-order corrections to Π. The curve (1) represents the relation $\tilde{\eta} = \eta$. The curve (2) represents $\tilde{\eta}$ in the three-dimensional case. The curve (3) represents $\tilde{\eta}$ in the two- or one-dimensional case. In the two-dimensional case, $\tilde{\eta}$ diverges as $|\log \eta|$ while it diverges as $\eta^{-1/2}$ in the one-dimensional case. The shaded area represents the critical region.

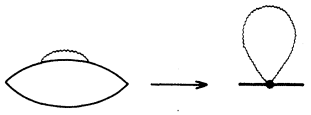

FIG. 5. Example of diagrammatic contraction: the first-order corrections to Π, schematically represented by the diagram on the left, yield the diagram on the right, the construction of which is explained in the text.

the two- and one-dimensional case when $\eta \to 0$.

This divergent behavior is indeed very unphysical and induces us to investigate the limits of validity of our approach. As pointed out in Sec. II, self-energy corrections to the electron Green's function will give rise to modifications of order $(x_i)^n$. On the other hand, the vertex corrections will give rise to corrections of order y_i^n [see Eqs. (1.8)–(1.10), which are essentially the quantities on the right of the + sign in the relations (3.5)–(3.7)].

IV. HIGHER-ORDER CORRECTIONS AND CRITICAL REGION

In this section, we shall consider the effect of higher-order diagrams in the evaluation of $\Pi(q, 0)$. Let Π_0 be the zeroth-order contribution to Π, i.e., the diagram (α) of Fig. 3. Let Π_1 be the first-order contribution to Π, i.e., the sum of the diagrams (β), (γ), (δ), (β'), (γ'), (δ') of Fig. 3. Let Π_2, Π_3, ... be the higher-order corrections to π. Π_2 and Π_3 are yielded by the sum of the diagrams drawn on Figs. 6 and 7, respectively. Those diagrams do not exhibit impurity scattering effects, which are supposed to be included in this symbolical representation. In order to evaluate those diagrams, it is readily seen that a convenient procedure consists in contracting the electron Green's-function loops into four points. This contraction is only possible because the electron momentum p is much larger than the momentum characteristic of the fluctuation. This means that the interaction among fluctuations due to the electron closed loop can be considered essentially as a local one.

For example, $\Pi_{1\beta}$ can be represented as seen on Fig. 5, where the external straight lines are simply present for the purpose of momentum conservation and are associated to a factor of 1 in view of the calculation. The point in Fig. 5, a "four-line vertex" (two incoming, two outgoing lines) corresponds to a factor Γ_3,

$$\Gamma_3 = \pi T N(0) \sum_{n=0}^{\infty} 1/|\omega_n|^3 . \tag{4.1}$$

The wavy line is a fluctuation line and corresponds to the summation

$$[1/N(0)]\, T \sum_{\vec{q}} [1/(\eta + \lambda q^2)] . \tag{4.2}$$

Similar contractions in the case of the diagrams of Figs. 6(a) and 7(a) yield the diagrams appearing in Figs. 6(b) and 7(b).

More generally, each "$2n$-line vertex" will be associated with a factor

$$\Gamma_{2n-1} \simeq \pi T N(0) \sum_{n>0}^{\infty} (1/|\omega_n|^{2n-1}) . \tag{4.3}$$

The precise coefficient in Γ_{2n-1} is yielded when one considers the expansion of the gap equation in powers of Δ.[30]

It should be pointed out here that the integration over q, performed in the case of the diagram on the right-hand side of Fig. 5, for example, yields a divergence when $|q| \to \infty$. However, if we go back to the microscopic expression of the diagram on the right-hand side of Fig. 5 (i.e., the sum of the diagrams $\Pi_{1\beta}$, $\Pi_{1\gamma}$, $\Pi_{1\delta}$, $\Pi_{1\beta'}$, $\Pi_{1\gamma'}$, $\Pi_{1\delta'}$, of Fig. 3), we see that the vertex corrections due to impurity scattering will suppress the divergence. Thus, in the case where divergences occur, one needs to go back to the microscopic expression, i.e., the expression in terms of the electronic Green's function. However, for an order-of-magnitude estimate, it will be sufficient to perform a dimensional analysis of such diagrams. On the contrary, an exact expression is yielded by the above-mentioned procedure in the case of non-diverging diagrams.

Finally, one must take into account the momentum conservation laws, as we can see from the consideration of the diagram $\Pi_{3\alpha}$ of Fig. 6. Its value is

$$\Pi_{3\alpha} \simeq \left(\pi T N(0) \sum_{0}^{\infty} \frac{1}{|\omega_n|^3}\right)^2 \frac{1}{[N(0)]^3}\, T^2 \times \sum_{\vec{q}_1, \vec{q}_2} \frac{1}{(\eta + \lambda q_1^2)(\eta + \lambda q_2^2)(\eta + \lambda q_3^2)} \quad (\vec{q}_1 + \vec{q}_2 + \vec{q}_3 = 0) . \tag{4.4}$$

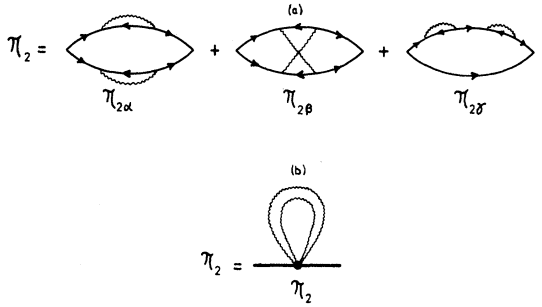

FIG. 6. Diagrammatic representation of Π_2: (a) before contraction, (b) after contraction.

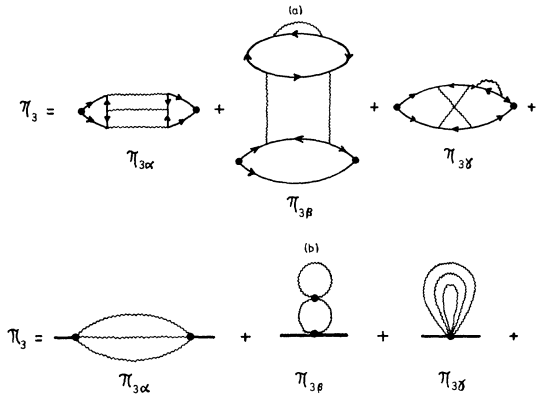

FIG. 7. Diagrammatic representation of Π_3: (a) before contraction, (b) after contraction.

Thus, we find

three dimensional:

$$\Pi_{3\alpha} = N(0)\left(\frac{7\zeta(3)}{8\pi^2}\right)\frac{16}{\pi^5}\frac{1}{[N(0)D\xi(0)]^2}\left(\ln\frac{1}{\eta}\right) , \tag{4.5}$$

two dimensional:

$$\Pi_{3\alpha} = N(0)\left(\frac{7\zeta(3)}{8\pi^2}\right)\frac{4C_1}{\pi^4}\frac{1}{[N(0)Dd]^2}\frac{1}{\eta} , \tag{4.6}$$

with

$$C_1 = \frac{4}{\sqrt{3}}\left(3\int_{\pi/3}^{\pi/2} d\theta\,[\ln(\sin\theta) + \tfrac{1}{4}\pi\ln 2]\right) , \tag{4.7}$$

one dimensional:

$$\Pi_{3\alpha} = N(0)\left(\frac{7\zeta(3)}{8\pi^2}\right)^2\frac{16}{\pi^2}\left(\frac{\xi(0)}{N(0)Dd^2}\right)^2\frac{1}{\eta^2}\left(1 - \frac{4}{3\sqrt{3}}\right). \tag{4.8}$$

As seen from the consideration of Fig. 6, such a contraction procedure is very convenient since it gives the result that the sum of the diagrams drawn in Fig. 6(a) yield the diagram in Fig. 6(b).

On the other hand, there is a very important difference between the diagrams $\Pi_{3\alpha}$ and $\Pi_{3\beta}$ of Fig. 7(b), and the diagram $\Pi_{3\gamma}$ of Fig. 7(b). Indeed, in the two-dimensional case

$$\begin{aligned} \Pi_{3\alpha} &\simeq N(0)a_2^2/\eta , \\ \Pi_{3\beta} &\simeq N(0)a_2^2[\ln(\eta^{-1})/\eta] , \end{aligned} \tag{4.9}$$

with

$$a_2 = 1/N(0)Dd . \tag{4.10}$$

On the contrary

$$\Pi_{3\gamma} \simeq N(0)[a_2\ln(\eta^{-1})]^3 . \tag{4.11}$$

Thus, when $\eta \to 0$, the most important contribution to Π_3 comes from $\Pi_{3\alpha}$ and $\Pi_{3\beta}$.

More generally, a very simple dimensional analysis shows that the most important contributions of a given order to Π will come from those diagrams containing the maximum number of the lowest-order vertices, i.e., Γ_3.

Consequently, it is now easy to retain the most important contributions to corrections of any order to Π. Thus, in the two-dimensional case, for example,

$$\begin{aligned} &\Pi_1 \sim a_2\ln(\eta^{-1}), \qquad \Pi_2 \sim (a_2\ln\eta)^2 , \\ &\Pi_3 \sim (a_2^2/\eta)\ln(1/\eta), \quad \Pi_4 \sim (a_2^3/\eta)\ln(\eta^{-1}) , \\ &\Pi_5 \sim (a_2^3/\eta^2) . \end{aligned} \tag{4.12}$$

Writing the renormalized value of η, $\tilde{\eta}$ as

$$\tilde{\eta} = [1/N(0)](1/g - \Pi) , \tag{4.13}$$

we obtain the following series, which can be written as follows, provided that we neglect constant numerical factors:

$$\begin{aligned} \tilde{\eta} \simeq \eta\,[1 &+ (a_2/\eta)\ln(\eta^{-1}) + a_2^2(\ln\eta)^2/\eta + (a_2^2/\eta^2)\ln(\eta^{-1}) \\ &+ (a_2^3/\eta^2)\ln(\eta^{-1}) + a_2^3/\eta^3 + \cdots] . \end{aligned} \tag{4.14}$$

Keeping in mind that a_2 is a small quantity, we retain in the above series only the most diverging terms, i.e., we can neglect all the corrections due to Π_2, Π_4, and Π_6 compared to those due to Π_1, Π_3, Π_5, ...

Finally, to a good approximation, we can write Eq. (4.14) in the form (where we have neglected logarithmic factors)

$$\tilde{\eta} \simeq \eta(1 + a_2/\eta + a_2^2/\eta^2 + a_2^3/\eta^3 + \cdots) . \tag{4.15}$$

Thus, as pointed out in Sec. I, our perturbation expansion will break down if [cf. Eq. (1.9)] $y \gtrsim 1$. Of course, the same result holds for the three- and one-dimensional cases. As the y_i are much larger than the x_i, we define the breakdown of the mean field theory by the conditions $y_i = 1$, which are conditions (1.11)–(1.13).

However, the dimensional analysis we have first used to obtain our results yields a further important conclusion. The diagrams we have considered above are exactly those appearing in the calculation of the fluctuation Green's function using the Ginzburg-Landau functional.[20] Thus

$$\mathcal{D}(r - r') = \int \delta\psi\psi^\dagger(r)\psi(r')e^{-\beta\mathcal{F}_{GL}(\psi,\psi^\dagger)} \Big/ \int \delta\psi e^{-\beta\mathcal{F}_{GL}(\psi,\psi^\dagger)} , \tag{4.16}$$

$$\mathcal{F}_{GL} = \frac{\pi N(0)}{8T}\int d^3r[\epsilon\,|\psi(r)|^2 + D\,|\vec{\nabla}\psi(r)|^2 + \tfrac{1}{2}b\,|\psi(r)|^4 + \tfrac{1}{6}b_2\,|\psi(r)|^6 + \cdots] \tag{4.17}$$

with $b = 7\zeta(3)/\pi^3 T$.

The above-mentioned analysis has shown us that the most important terms were obtained by the diagrams containing the maximum number of vertices Γ_3. Consequently, in view of the determination of $\mathfrak{D}$, we are allowed to neglect terms of higher order than $|\psi|^4$ in the expansion of $\mathfrak{F}_{GL}$ in powers of ψ. Now, we shall comment on the above results in the conclusion.

V. CONCLUSION

We have shown in Secs. II–IV the results presented in the Introduction.

In particular, we have shown that the corrections to the mean field theory are generally small, except when one gets close to the critical region.[31]

The criterion we have obtained for the onset of the critical region $\eta = \eta_{ci}$ is the same as the one proposed earlier by Ginzburg,[16] Ferrell,[20] and Tsuzuki.[22] On the other hand, it differs from the one proposed by Brout or by Fischer,[17,19] and also from an earlier estimate by Ferrell and Schmidt.[18]

It is not surprising that we find the same result as Ferrell,[20] since we present essentially a microscopical justification of his approach. We find also the same result as Tsuzuki[22] since this author considers the diagram $\Pi_{3\alpha}$ of Fig. 7 to deduce his criterion. However, our analysis shows that the conclusion obtained by Tsuzuki is also true when one examines the higher-order diagrams.

As far as the comparison with experimental data is concerned, our criterion (1.12) seems to work reasonably well in the case of Glover's experiment. Indeed using numerical values relevant to Ref. 2 ($l \sim 10$ Å, $d \sim 100$ Å), (1.12) yields $\eta_c \sim 10^{-3}$, which can account reasonably well for the deviation from the $T_c/(T - T_c)$ behavior of the electrical conductivity above the transition temperature.

Some properties of superconducting samples above their transition temperature (such as the electrical conductivity, for example) depend on $\tilde{\eta}$. From the measurements of such properties in the "classical" region (by fitting the divergence of the electrical conductivity to the Aslamasov-Larkin expression, for example) one can deduce a value of the critical temperature T_c^*. As we have seen, the renormalization effects on η due to fluctuations are very small in the classical region. However, they might affect the values of T_c^*. In the two-dimensional case, the shift $\Delta T_c = T_c^* - T_c$ due to the fluctuations is only

$$\Delta T_c/T_c = -(2.4/p_0^2 ld)[\ln(1/\eta) - 1] \quad . \tag{5.1}$$

In the case of the experiments by Glover,[2] this last relation can be written

$$\Delta T_c/T_c < 1\,\text{Å}/d \quad , \tag{5.2}$$

where d is in Å units.

However, the relation (5.2) gives too small a value for the ratio $|\Delta T_c/T_c|$ compared to the one observed experimentally.[25] The experimental shift seems thus to be extrinsic to fluctuation effects, as already noticed by Ferrell.[20] On the other hand this shift seems to be well accounted for in terms of proximity effects.[26] At the film surface, which is in contact with an insulator, the logarithmic derivative of the order parameter is given by

$$\frac{d}{dx}\ln[\psi(x)] \simeq \frac{a}{\xi^2} \quad ,$$

where a is of the order of interatomic distance and x is the distance from the surface of the film. Hence the virtual order parameter acquires a slight spatial dependence across the film thickness resulting in a shift of the transition temperature. Thus the proximity effect introduces a pair-breaking parameter into the theory of the electrical conductivity which results in a cancellation of the divergence associated with the so-called Maki diagram[11,13]. This seems to explain why the Aslamasov-Larkin term[9] only gives a good account of the experimental data observed in the above-mentioned experiment.

Finally, we propose the following procedure for the analysis of the thermodynamical properties in the critical region.

(a) Determine $\mathfrak{D}$ from the relation (5.16), where

$$\mathfrak{F}_{GL} = (\pi/8T)\int d^3r\,(\epsilon|\psi|^2 + D|\vec{\nabla}\psi|^2 + \tfrac{1}{2}b|\psi|^4) \quad .$$

(b) Inject the value of $\mathfrak{D}$ into the calculation of G performed in the same way as in Sec. II.

Since there is a one-to-one correspondence between the diagrams generated by the Ginzburg-Landau functional given above and those for the interacting Bose system, we can say that the critical behavior of the fluctuations is identical in these two systems. Making use of Migdal's result[32] in his recent analysis of the Bose system, we can say that the critical behavior of a superconductor is described by scaling laws. However, the critical exponents can only be determined by a more detailed numerical analysis.

ACKNOWLEDGMENTS

We thank M. T. Béal-Monod, M. Cyrot, P. G. de Gennes, and the members of the experimental Orsay Group on superconductivity for many helpful discussions. We thank also E. Abrahams for sending us the report of their work prior to publication. One of us (K. M.) is grateful to Centre National de la Recherche Scientifique for the financial support.

APPENDIX A: CALCULATION OF $\Sigma_a(\omega_n, \vec{p})$

The term Σ_a is the self-energy diagram in Fig. 2(a). Σ_a obtained by

$$\Sigma_a(\omega_n, \vec{p}) = T\sum_{\nu}\sum_{q} \frac{\theta(\omega_n, \omega_{n+\nu})}{i\tilde{\omega}_{n+\nu} + \xi_{p+q}} \frac{(|2\omega_n + \omega_\nu| + \tau^{-1})^2}{(|2\omega_n + \omega_\nu| + Dq^2)^2} \frac{1}{N(0)(\eta + \lambda q^2 + \pi|\omega_\nu|/8T)} , \tag{A1}$$

$$\Sigma_a(\omega_n, p) = \frac{T}{N(0)}\sum_{q}\left(\sum_{\nu=0}^{\infty} \frac{1}{i\tilde{\omega}_{n+\nu} + \xi_{p+q}} \frac{(|2\omega_n| + \omega_\nu + \tau^{-1})^2}{(|2\omega_n| + \omega_\nu + Dq^2)^2} \frac{1}{\eta + \lambda q^2 + \pi\omega_\nu/8T}\right.$$

$$\left. + \sum_{\nu=1}^{n-1} \frac{1}{i\tilde{\omega}_{n-\nu} + \xi_{p+q}} \frac{(|2\omega_n| - \omega_\nu)^2}{(|2\omega_n| - \omega_\nu + Dq^2)^2} \frac{1}{\eta + \lambda q^2 + \pi\omega_\nu/8T}\right) , \tag{A2}$$

$$\Sigma_a(\omega_n, p) \simeq \frac{(2\tilde{\omega}_n)^2}{i\tilde{\omega}_n + \xi_p} \frac{4T}{\pi^2 N(0)} \sum_{q}\left(\frac{1}{(|2\omega_n| + \epsilon)^2}\left[\psi\left(\frac{|2\omega_n| + Dq^2}{2\pi T}\right) - \psi\left(\frac{\epsilon + Dq^2}{2\pi T}\right)\right] + \frac{1}{(|2\omega_n| + \epsilon + 2Dq^2)^2}\right.$$

$$\times\left[\psi\left(\frac{|2\omega_n| + Dq^2}{2\pi T}\right) - \psi\left(1 + \frac{\epsilon + Dq^2}{2\pi T}\right) + \psi\left(\tfrac{1}{2} + \frac{|\omega_n| + Dq^2 + \epsilon}{2\pi T}\right) - \psi\left(\tfrac{1}{2} + \frac{|\omega_n| + Dq^2}{2\pi T}\right)\right]$$

$$- \frac{1}{2\pi T}\left\{\frac{1}{|2\omega_n| + \epsilon} \psi'\left(\frac{|2\omega_n| + Dq^2}{2\pi T}\right) + \frac{1}{|2\omega_n| + \epsilon + 2Dq^2}\right.$$

$$\left.\left. \times \left[\psi'\left(\frac{|2\omega_n| + Dq^2}{2\pi T}\right) - \psi'\left(\tfrac{1}{2} + \frac{|\omega_n| + Dq^2}{2\pi T}\right)\right]\right\}\right) . \tag{A3}$$

In (A3), ψ and ψ' are, respectively, the diagamma and trigamma functions and $\epsilon = (8T/\pi)\eta$. Here, we have neglected the corrections of higher order in $\tau\omega_\nu$ and lq. Furthermore, if we retain only the pole terms coming from the polygamma functions, which give rise to the singular contributions, we can simplify (A3) and we have

$$\Sigma_a(\omega_n, \vec{p}) \simeq \frac{(2\tilde{\omega}_n)^2}{i\tilde{\omega}_n + \xi_p} \frac{8T}{\pi N(0)} \sum_{q}\left[\frac{1}{(2|\omega_n| + \epsilon)^2} \frac{1}{\epsilon + Dq^2}\right.$$

$$- \frac{2}{2|\omega_n| + \epsilon + 2Dq^2} - \frac{2}{(|2\omega_n| + \epsilon)}$$

$$\left. \times \frac{1}{(|2\omega_n| + \epsilon + 2Dq^2)^2}\right] , \tag{A4}$$

which is essentially Eqs. (2.10) and (2.11).

APPENDIX B: CALCULATION OF $\Pi_1(0, q)$

Making use of the expression of Σ_a we have just obtained it is easy to express the diagram $\Pi_{1\beta}$ of Fig. 3. Thus

$$\Pi_{1\beta} = T\sum_{n=-\infty}^{+\infty} \Lambda^2(\omega_n, \omega_n; q)$$

$$\times \int \frac{d^3p}{(2\pi)^3} [G_0(\omega_n, \vec{p})]^2 \Sigma_a(\omega_n, \vec{p}) G_0(-\omega_n, \vec{p})$$

$$= T\sum_{n=-\infty}^{+\infty} \Lambda^2(\omega_n, \omega_n; q)$$

$$\times \int \frac{d^3p}{(2\pi)^3} \frac{1}{(i\tilde{\omega}_n - \xi_p)^2} \frac{1}{(i\tilde{\omega}_n + \xi_p)^2} F(|\omega_n|)$$

$$= -4\pi T N(0) \sum_{n} \frac{\Lambda^2(\omega_n, \omega_n; q)}{(2\tilde{\omega}_n)^3} F(|\omega_n|) . \tag{B1}$$

In (B1), $F(|\omega_n|)$ is given by the relation (2.11).

On the other hand, the contribution to the diagram $\Pi_{1\gamma}$ can be written as

$$\Pi_{1\gamma} = n|u|^2 T\sum_n \Lambda^2(\omega_n, \omega_n; q)$$

$$\times \int \frac{d^3q'}{(2\pi)^3} \frac{1}{(i\tilde{\omega}_n - \xi_{p'})^2} \Sigma_a(\omega_n, \vec{p}')$$

$$\times \int \frac{d^3p}{(2\pi)^3} \frac{1}{(i\tilde{\omega}_n - \xi_p)^2 (i\tilde{\omega}_n + \xi_p)}$$

$$= N(0) \frac{T}{2\tau} \sum_n \frac{4\pi}{(2\tilde{\omega}_n)^4} F(|\omega_n|) \Lambda^2(\omega_n, \omega_n; q) , \tag{B2}$$

where we have assumed an isotropic scattering potential and we have made use of the relation

$$1/\tau = 2\pi n|u|^2 N(0) .$$

Finally, the diagram $\Pi_{1\delta}$ yields

$$\Pi_{1\delta} = Tn|u|^2 \sum_n \left(\int \frac{d^3p}{(2\pi)^3} \frac{1}{(i\tilde{\omega}_n + \xi_p)^2} \frac{1}{i\tilde{\omega}_n - \xi_p} \right)^2 \times \Lambda^2(\omega_n, \omega_n; q) F(|\omega_n|)$$

$$= TN(0) \sum_n \frac{4\pi\Lambda^2(\omega_n, \omega_n, q)}{2\tau(2\tilde{\omega}_n)^4} F(|\omega_n|) \quad . \quad \text{(B3)}$$

If we sum $\Pi_{1\beta}$, $\Pi_{1\gamma}$, $\Pi_{1\delta}$ and multiply by a factor of 2 to include the effect of $\Pi'_{1\beta}$, $\Pi'_{1\gamma}$, $\Pi'_{1\delta}$, we obtain

$$\Pi_1 = -8\pi TN(0) \sum_n \frac{\Lambda^2(\omega_n, \omega_n; q)}{(2|\tilde{\omega}_n|)^3} \times \left(1 - \frac{1}{2\tau|\tilde{\omega}_n|}\right) F(|\omega_n|) \ ,$$

which yields the approximate relation (3.1).

It is worthwhile to note here that Π_1 is much more easily calculated in terms of the Ginzburg-Landau functional through the consideration of the diagram on the right-hand side of Fig. 5.

---

*Permanent address: Laboratoire d' Electronique et de Physique Appliquée, B. P. 15, 94, Limeil-Brévannes, France.

†Permanent address: Department of Physics, Tôhoku University, Sendai, Japan.

‡Associé au Centre National de la Recherche Scientifique, 91-Orsay, France.

[1]J. S. Shier and D. M. Ginsberg, Phys. Rev. 147, 384 (1966).

[2]R. E. Glover, Phys. Letters 25A, 542 (1967); R. R. Hake, Phys. Rev. Letters 23, 1105 (1969).

[3]M. Strongin, O. F. Kammerer, J. Crow, R. S. Thompson, and H. L. Fine, Phys. Rev. Letters 20, 922 (1968).

[4]J. P. Gollub, M. R. Beasley, R. S. Newbower, and M. Tinkham, Phys. Rev. Letters 22, 1288 (1969); L. L. Want-Hull and J. E. Mercereau, in Proceedings of the International Conference on the Science of Superconductivity, Stanford, 1969 (unpublished).

[5]R. W. Cohen, B. Abeles, and C. R. Fusellier, Phys. Rev. Letters 23, 377 (1969).

[6]A. Lehoczky and C. V. Briscoe, Phys. Rev. Letters 23, 695 (1969).

[7]B. Serin, R. O. Smith, and T. Mizusaki, in Proceedings of the International Conference on the Science of Superconductivity, Stanford, 1969 (unpublished).

[8]R. J. Warburton and W. W. Webb, in Ref. 7.

[9]L. G. Aslamasov and A. I. Larkin, Phys. Letters 26A, 238 (1968).

[10]H. Schmidt, Z. Physik 216, 336 (1968); B. R. Patton, V. Ambegaokar, and J. Wilkins, Solid State Commun. 7, 1287 (1969).

[11]K. Maki, Progr. Theoret. Phys. (Kyoto) 39, 897 (1968).

[12]P. Fulde and K. Maki, Phys. Kondsierten Materie 8, 371 (1969).

[13]R. S. Thompson, Ref. 7.

[14]E. Abrahams, R. E. Prange, and M. J. Stephen, in Ref. 7; K. Maki, Low Temp. Phys. 1, 513 (1969); K. Usadel, Z. Physik 227, 260 (1969); H. J. Mikeska and H. Schmidt (report of work prior to publication).

[15]E. Abrahams, M. Redi, and J. W. F. Woo, Phys. Rev. (to be published).

[16]V. L. Ginzburg, Fiz. Tverd. Tela 2, 2031 (1960) [Soviet Phys. Solid State 2, 1824 (1960)].

[17]R. Brout, Phys. Rev. 118, 1009 (1960).

[18]R. Ferrell and H. Schmidt, Phys. Letters 25A, 544 (1967).

[19]For a review paper on the breakdown of the mean field theory, see P. C. Hohenberg, in *Proceedings of the Conference on Fluctuations in Superconductors*, edited by W. S. Goree and F. Chilton (Stanford Research Institute, Stanford, Calif., 1968), p. 305.

[20]R. Ferrell, in Ref. 19, p. 239; L. Gunther and L. Gruenberg (report of work prior to publication).

[21]K. Maki, Progr. Theoret. Phys. (Kyoto) 40, 193 (1968).

[22]T. Tsuzuki, Progr. Theoret. Phys. (Kyoto), 41, 296 (1969).

[23]L. P. Kadanoff and G. Laramore, Phys. Rev. 175, 579 (1968).

[24]We use units in which $\hbar = k_B = 1$.

[25]D. G. Naugle and R. E. Glover, Phys. Letters 28A, 611 (1969).

[26]R. E. Glover, D. G. Naugle, and X. Moormann, in Ref. 7.

[27]See, for example, A. A. Abrikosov, L. P. Gorkov, and I. E. Dzialoshinski, *Methods of Quantum Field Theory in Statistical Physics* (Prentice-Hall, Englewood Cliffs, N. J., 1964), p. 325.

[28]C. Caroli and K. Maki, Phys. Rev. 159, 306 (1967).

[29]L. P. Gor'kov and G. M. Eliashberg, Zh. Eksperim. i Teor. Fiz. 54, 612 (1968); 55, 2430 (1968) [Soviet Phys. JETP 27, 328 (1968); 28, 1291 (1969)].

[30]See, for example, K. Maki, *Treatise on Superconductivity*, edited by R. D. Parks (Marcel Dekker, New York, 1969).

[31]As pointed out to us by Dr. M. T. Béal-Monod, a similar conclusion seems to be also valid in the case of locally quasi-magnetic-systems. Thus, self-consistent treatments in which self-energy effects are only taken into account will yield erroneous results [cf. M. T. Béal-Monod and D. L. Mills, Phys. Rev. Letters 24, 225 (1970)].

[32]A. A. Migdal, Zh. Eksperim. i Teor. Fiz. 55, 1964 (1968) [Soviet Phys. JETP 28, 1036 (1969)].